Microchim Acta (2016) 183:1543–1551
DOI 10.1007/s00604-016-1763-1

ORIGINAL PAPER

A glassy carbon electrode modified with an amphiphilic, electroactive and photosensitive polymer and with multi-walled carbon nanotubes for simultaneous determination of dopamine and paracetamol

Ren Liu[1] · Xuebiao Zeng[1] · Jingcheng Liu[1] · Jing Luo[1] · Yuanyi Zheng[1] · Xiaoya Liu[1]

Received: 11 October 2015 / Accepted: 21 January 2016 / Published online: 17 March 2016

Abstract The article describes an electrochemical sensor for simultaneous determination of dopamine (DA) and paracetamol (PAT). It is based on the use of an electroactive polymer (referred to as BPVCM) to functionalize multi-walled carbon nanotubes. BPVCM is a branched amphiphilic photosensitive and electroactive polymer that was obtained by copolymerization of a vinyl benzylcarbazole, maleic acid anhydride, 4-vinylbenzylthiol and a vinylbenzyloxycoumarin. BPVCM efficiently disperses MWCNT in aqueous solution. The electropolymerization of the carbazole moieties of the BPVCM enhances the current response. It also facilitates electron transfer in the MWCNT-BPVCM hybrid as evidenced by cyclic voltammetry and electrochemical impedance spectroscopy. A glassy carbon electrode modified with the nanocomposite displays outstanding electrocatalytic activity towards DA and PAT. DA can be determined, best at a working voltage of 0.2 V (vs. SCE), in the 5 to 1000 μM concentration range with a 2.3 μM detection limit. PAT can be determined in parallel, at a working voltage of 0.39 V (vs. SCE), in the same concentration range with a 3.5 μM detection limit. This analytical range of this method is wider than that of most alternative methods.

Keywords Electrochemical sensor · Neutrotransmitter · Electrochemical polymerization · Cyclic voltammetry · Electrochemical impedance spectroscopy

Introduction

Dopamine (DA) is one of the main neurotransmitter in mammalian metabolism and it plays a vital physiological role in our central nervous, renal, hormonal and cardiovascular systems [1]. The low concentration level of DA may cause neurological disorders such as schizophrenia, Parkinson's disease and HIV infection. So it is of great clinical importance to measure DA level for diagnosing these diseases. Acetaminophen, *N*-acetyl-*p*-aminophenol or paracetamol (PAT) is an important drug used for antipyretics and analgesics against for reduction of fevers, headaches and other aches or pains [2]. However, overdoses of PAT result in an accumulation of toxic metabolites, and can be fatal. In addition, PAT is known to interfere with the measurements of DA in the real samples, so it is quite desirable to develop new materials which can resolve the two competing signals of DA and PAT. Several methods for determination of DA and PAT have been employed such as high performance liquid chromatography, mass spectroscopy, spectrofluorimetry and capillary zone electrophoresis [3–17]. However, these methods suffer from some disadvantages including time consuming, high cost and the requirement for pretreatment step.

The electrochemical method has become a powerful technique because of simplicity, high sensitivity, low cost and short measurement time. However, owing to the similar chemical structures of DA and PAT, their redox peaks at unmodified electrodes are quite close to each other, which leads to a poor detection selectivity. Up to now, a wide range of nanomaterials with good conductivity or electrocatalytic activity have been

Electronic supplementary material The online version of this article (doi:10.1007/s00604-016-1763-1) contains supplementary material, which is available to authorized users.

✉ Xiaoya Liu
lxy@jiangnan.edu.cn; lxyjiangnan@126.com

[1] The Key Laboratory of Food Colloids and Biotechnology, Ministry of Education, School of Chemical and Material Engineering, Jiangnan University, Wuxi 214122, People's Republic of China

employed to modify electrode to determine DA and PAT simultaneously to solve these problems [5–10]. For example, Zhang et al. prepared porous gold nanosheets modified glassy carbon electrode (GCE) by one-step electrodeposition using N-methylimidazole as a growth-directing agent, which displayed individual and simultaneous differential pulse voltammetric determination of dopamine and acetaminophen in the presence of ascorbic acid [5]. Zirconium nanoparticles decorated reduced graphene oxide has also been employed as an electrode material for simultaneous sensing dopamine and acetaminophen [9]. But the detection range and detection limit of these nanocomposites modified electrode for DA and PAT still needs to be improved. Therefore, it is still a challenge to explore novel electrode materials for the simultaneous determination of DA and PAT with wider linear range and lower detection limit.

Carbon nanotubes (CNT) have attracted a great deal of attention due to their inherently outstanding electronic and thermal conductivity, particularly for application in advanced materials, including transistors, photovoltaic devices, supercapacitors, solar cells and electrochemical sensors [18]. The electrodes modified with CNT have been proved to possess extraordinary properties over the non-modified electrodes including highly effective surface areas, outstanding electrical properties, high porosity and reactive sites [19, 20]. However, extended van der Waals interactions between CNT lead to aggregation into insoluble bundles which put a great obstacle in its process ability. Although stable and homogenous CNT dispersion have been achieved using polymer or surfactant as dispersant [21–24], the electrical property of CNT was sacrificed due to the presence of the insulating dispersant, which is not suitable for application in electrochemical devices considering the interfacial resistor [25, 26]. The CNT-polymer modified electrodes have low sensitivity and limited linear range because of the insulating properties of polymer.

Recently, we have reported the functionalization of MWCNT with a branched amphiphilic photo-sensitive and electroactive polymer (BPVCM), and the preliminary results showed that resulted MWCNT-BPVCM composite has a significant improvement in the electrical property [27]. A more detailed study about the change of the electrical property of MWCNT-BPVCM nanocomposite after the electro-polymerization of carbazole moieties is described in this work. With the synergistic effect, the resulted MWCNT-BPVCM composite was used to modify the glass carbon electrode (GCE) and demonstrated to be an effective material for the fabrication of electrochemical sensor for the simultaneous determination of DA and PAT. The electrochemical behavior of the fabricated sensor (MWCNT-BPVCM-*e*/GCE) towards DA and PAT was investigated by cyclic voltammetry (CV). Two corresponding well-defined redox peaks with well separated peak potentials and enhanced peak currents were obtained which allowed the simultaneous detection of DA and PAT with high sensitivity. More interestingly, the interference of ascorbic acid (AA) is also effectively avoided.

Experimental

Chemicals and reagents

Dopamine (DA), paracetamol (PAT) and ascorbic acid (AA) were obtained from Shanghai Aladdin Reagent. Multi-walled carbon nanotubes (10–20 nm in diameter, length of 10–30 μm, > 95 wt%) were purchased from Chengdu Organic Chemicals Institute, Chinese Academy of Sciences (http://timesnano.cnpowder.com.cn). All the other chemical reagents used were of analytical grade and used as received. Prior to the analysis, the dopamine hydrochloride injection (10 $mg \cdot mL^{-1}$, Shanghai Harvest pharmaceutical Co., Ltd, www.shharvest.com) and paracetamol tablet (0.3 g, Tianjin Jiansheng pharmaceutical Co., Ltd, http://tjjs2015.tecenet.com) were diluted with pH 7.0 (0.1 M PBS) solution. All solutions were prepared with ultrapure fresh water from a NW Ultra-pure Water System (Specific resistivity > 18.2 MΩ•cm, Heal Force, Hong Kong). The branched amphiphilic photo-sensitive and electroactive polymer (BPVCM) was synthesized from 9-(4-vinylbenzyl)-9*H*-carbazole (VCz), maleic anhydride (MA), 4-vinyl benzyl thiol (VBT) and 7-(4-vinylbenzyloxy)-4-methyl coumarin (VM) according to the previous literature [27].

Apparatus

The surface morphology of the MWCNT-BPVCM-*e*/GCE was observed using a Hitachi S-4800 field emission scanning electron microscope (FESEM) operating at 1 KV. Transmission electron microscopy (TEM) study was examined using a JEOL-2010 transmission electron microscope (www.jeol.co.jp/cn/). Thermogravimetric analysis (TGA) was performed under a nitrogen atmosphere using a thermogravimetric analyzer (Mettler Toledo instrument, TGA/1100SF, www.mtchina.com) operated at a heating rate of 10 $°C \cdot min^{-1}$ from 25 to 600 °C. Electrochemical impedance spectroscopy (EIS) (CHI 660C electrochemical analyzer, Chenhua Corp., Shanghai, China) was used to investigate the impedance properties of the MWCNT-BPVCM nanocomposite films. Cyclic voltammetry (CV) were carried out on a Epsilon electrochemical workstation (BAS, USA, www.basvs.com) using a three-electrode system. The glassy carbon electrode (GCE, 3 mm diameter; Aida, Tianjin, China, www.tjaida.cn) was used as the working electrode, a platinum wire electrode (Aida) was used as the counter electrode and a saturated calomel electrode (SCE, Aida) as the reference electrode. All potentials applied to the working electrode were

referred to SCE and all electrochemical detection experiments were carried out at room temperature.

Preparation

Preparation of BPVCM functionalized MWCNT aqueous dispersion

The BPVCM copolymer and MWCNT-BPVCM nanocomposite in aqueous solution was prepared as described previously [27]. Typically, pristine MWCNT (0.8–8 mg) were added into 1 mL of DMF solution containing 2 mg of the BPVCM polymer with the aid of sonication for 1 h. Then, 9 mL of deionized water was added dropwise at 0.1 $mL \cdot min^{-1}$ to induce the self-assembly of BPVCM copolymer around MWCNT, leading to aqueous dispersion of MWCNT-BPVCM.

Preparation of MWCNT-BPVCM nanocomposite modified GCE

The bare GCE was carefully polished with 0.5 μm Al_2O_3 powder and polishing cloth, and then rinsed by sonication in ethanol and ultrapure fresh water, finally dried at the room temperature. 5 μL of MWCNT-BPVCM dispersion was dropped on a pretreated bare GCE surface and dried in nitrogen atmosphere at 25 °C.

The obtained MWCNT-BPVCM film was then electrochemically cross-linked using CV. CV experiments were carried out on an Epsilon electrochemical workstation using a three-electrode system from a solution of 0.1 M $LiClO_4$ dissolved in acetonitrile. The MWCNT-BPVCM/GCE was used as the working electrode. Electrochemical cross-linking of MWCNT-BPVCM nanocomposite film was accomplished by repeatedly cycling the electrode potential between the potential range of 0 to 1.5 V for 20 cycles at a potential scan rate of 100 $mV \cdot s^{-1}$ [28]. The highly cross-linked nanocomposite film was thoroughly washed with ultrapure fresh water and was dried before its analysis (Fig. 1).

Results and discussion

Choice of Materials

To achieve an efficient dispersing effect for MWCNT, branched polymers BPVCM was synthesized considering their attractive features such as the multiple end groups, improved solubility and lower solution viscosity. In addition, the amphiphilic copolymer containing coumarin groups can undergo crosslinking under UV-irradiation and encapsulate MWCNTs in the crosslinked copolymer micelles, which have been demonstrated to improve the stability of the obtained MWCNT suspension [27]. Furthermore, the reported polymer dispersants used to disperse MWCNT were normally insulate and led to the decrease of electrical conductivity of MWCNT, which is quite disadvantageous for its application in electrochemical device. So electroactive polymers are more desirable to modify carbon nanotubes. Based on the above considerations, a branched amphiphilic copolymer with photosensitivity and electroactivity has been designed and prepared here through simple one-pot free-radical polymerization and successfully been employed to noncovalently disperse MWCNT. Maleic anhydride (MA), 7-(4-vinylbenzyloxy)-4-methyl coumarin (VM), vinylcarbazole (VCz) and 4-vinylbenzyl thiol (VBT) were employed as hydrophilic, photosensitive, electroactive, and chain transfer monomers, respectively. 4-vinylbenzyl thiol (VBT) containing a polymerizable vinyl group and a chain transferring/initiating thiol group was used as chain transfer monomer, which can initiate the chain transfer/initiating reaction and produce the branched macromolecules [27].

Characterization of MWCNT-BPVCM nanocomposite

The surface morphology of MWCNT-BPVCM nanocomposite was analyzed by TEM. The TEM image of pristine MWCNT (Fig. 2a) depicts tubular structures of diameter ranging from 10 to 20 nm. For MWCNT-BPVCM nanocomposite, a great number of uniform spherical micelles were observed wrapping along the sidewalls of MWCNT which matched the outer of MWCNT in the range of 80–120 nm (Fig. 2b). This observation demonstrates the successful functionalization of MWCNT by BPVCM, which leads to debundling and well-separated MWCNT.

The amount of BPVCM modified to the surface of MWCNT, defined as the ratio of the mass of the immobilized BPVCM to that of the MWCNT-BPVCM nanocomposite, was estimated from TGA (Fig. S1). As shown in Fig. S1, MWCNT-BPVCM exhibited major weight loss in the temperature range of 300–500 °C due to the degradation of BPVCM adsorbed onto the sidewalls of MWCNT, and the amount of BPVCM in the composite is about 40 wt.%. The inset of Fig. S1 shows the dispersion behavior of pristine MWCNT and MWCNT-BPVCM in water (the concentration of MWCNT is 0.08 $mg \cdot mL^{-1}$) after 30 days. MWCNT without BPVCM entangled and precipitated at the bottom of the sample bottle, while BPVCM functionalized MWCNT exhibited black-colored ink-like dispersion and no precipitation was observed, which vividly confirmed the improved stability of the dispersion.

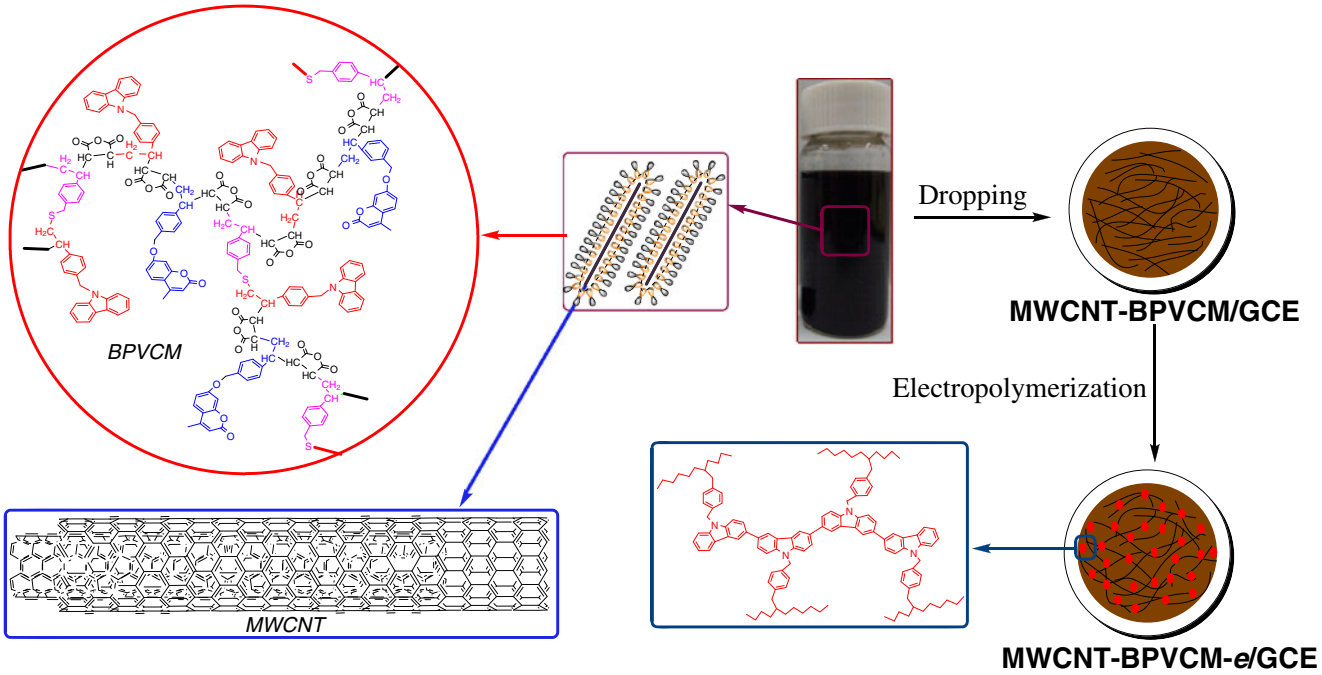

Fig. 1 Schematic illustration of preparation of MWCNT-BPVCM nanocomposite cross-linked film on the glassy carbon electrode surface

Electrochemical impedance spectra and cyclic voltammograms of MWCNT-BPVCM/GCE with different concentration of MWCNT

Electrochemical impedance spectroscopy (EIS) provides useful information on the impedance changes of the modified electrode surface to characterize the stepwise construction process of the sensor [29]. The impedance spectrum normally included a semicircle portion at higher frequencies and a linear portion at lower frequencies. The semicircle portion at higher frequencies corresponds to the charge transfer resistance (R_{ct}), and the linear portion at lower frequencies corresponds to the diffusion process. Fig. S2A shows representative impedance spectra of MWCNT-BPVCM/GCE with different concentration of MWCNT in 0.1 M KCl containing 5 mM $Fe(CN)_6^{3-/4-}$. As shown in Fig. S2A, as the concentration of MWCNT (0.08–0.80 $mg \cdot mL^{-1}$) in MWCNT-BPVCM increased, the R_{ct} decreases obviously. This could be explained by the fact that the higher concentration of MWCNT in the MWCNT-BPVCM composite, the more amount of MWCNT is dropped on the surface of GCE, and thus the better the electrical property of the MWCNT-BPVCM hybrid film. The improved electrical performance can be further demonstrated by CV. As presented in Fig. S2B, we can see clearly an increase in the amperometric response and a decrease in the peak-to-peak separation between the cathodic and anodic peaks of the redox probe with increasing the concentration of MWCNT, further demonstrating that more MWCNT can accelerate the access of the redox probe to the electrode surface.

Effect of electropolymerization of carbazole units of MWCNT-BPVCM nanocomposite on the GCE

Carbazole is an electro-active unit that readily electropolymerize to form large conjugate structure [28]. So, for MWCNT-BPVCM composite, the electropolymerization of

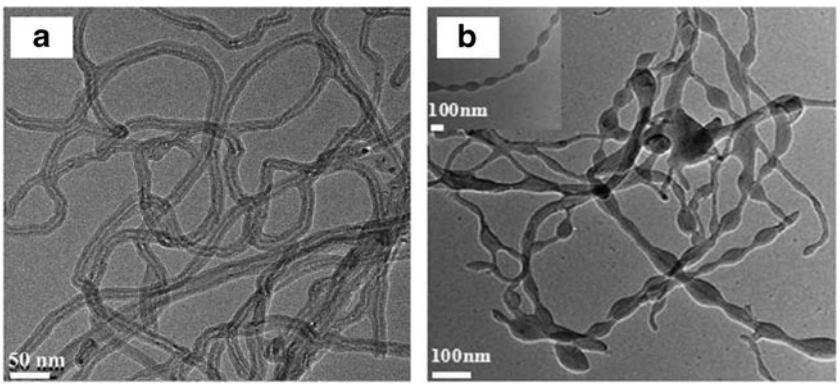

Fig. 2 TEM images of MWCNT (**a**) and MWCNT-BPVCM nanocomposite (**b**)

carbazole creates a π-conjugated conductive network containing both inter- and intramolecular cross-linkages between the pendant carbazole units (the inset of Fig. S3) on the surface of MWCNT and thus enhance the electrical properties of MWCNT-BPVCM nanocomposite. The electrochemical cross-linking of the carbazole moieties was recorded using 0.1 M $LiClO_4$ as supporting electrolytes in ACN as shown in Fig. S3. The anodic peak potential of the nanocomposite is 1.30 V after the first electropolymerization cycle and it shifts to 1.25 V after twenty cycles, which is related to an increase in conjugation as the chains grow thus facilitating the oxidation reaction. And there is nearly no change about the anodic peak potential after twenty cycles which confirms the complete electropolymerization of carbazole units.

The impedance spectra of MWCNT-BPVCM/GCE before and after electropolymerization (MWCNT-BPVCM/GCE and MWCNT-BPVCM-*e*/GCE) have been investigated and discussed in our previous work [27]. Bare GCE presents a small semicircle domain with the value of 600 ± 15 Ω (R_{ct}). After modified by the MWCNT-BPVCM nanocomposite, the R_{ct} increased to 2000 ± 50 Ω. [27]. The large R_{ct} value for MWCNT-BPVCM should be attributed to the presence of the insulating BPVCM. In contrast, after electropolymerization, the MWCNT-BPVCM-*e*/GCE presented nearly a linear portion with a significantly reduced R_{ct} (450 ± 20Ω) which is quite similar to that of pristine MWCNT. The almost four times decreased R_{ct} demonstrated that electropolymerization of carbazole has created a conductive network of nanocomposite on the surface of electrode which formed high electron conduction pathways between the electrode and electrolyte. This result obviously confirmed that the MWCNT-BPVCM nanocomposite after electropolymerization improved the conductivity of the hybrid film. And the electrical properties of a bare GCE, MWCNT-BPVCM nanocomposite modified GCE before and after electropolymerization were further compared by CV using $Fe(CN)_6^{3-/4-}$ as probe. Compared to MWCNT-BPVCM nanocomposite before electropolymerization, the composite after electropolymerization (MWCNT-BPVCM-*e*) showed an almost two-fold increase in the peak current response. And a decrease in the peak to peak separation between the cathodic and anodic waves of the redox probe from 200 to 100 mV was also observed, further confirming the improved electrical properties.

Cyclic voltammograms of DA and PAT at MWCNT-BPVCM nanocomposite modified GCE

With the synergistic effect of MWCNT and the electropolymerized BPVCM, the resulted MWCNT-BPVCM composite modified electrode was employed for the simultaneous determination of DA and PAT. The electrochemical behavior of DA and PAT on MWCNT-BPVCM modified electrode was investigated by CV. Fig. 3 shows the cyclic voltammograms of 100 μM DA and PAT on MWCNT-BPVCM modified GCE before and after electropolymerization. For comparison, the responses of DA and PAT on bare GCE were also provided. As shown in Fig. 3, the peaks of DA and PAT on bare GCE are indistinguishable and overlap with each other. With the modification by MWCNT-BPVCM, the peak current of DA and PAT increased greatly and the peak-potential separation between the oxidation peak potential (E_{pa}) and the reduction peak potential (E_{pc}) becomes smaller. But the peaks of DA and PAT are still inseparable. In contrast, after electropolymerization, two well-defined redox peaks corresponding to DA and PAT with well separated peak potentials were obtained. The anodic peak potentials for DA and PAT were at 220 mV and 415 mV, and their cathodic potentials were at 165 mV and 330 mV respectively, indicating an anodic peak potential separation (Epa) of 195 mV and an cathodic peak potential separation of 165 mV, which was favorable for the simultaneous detection of DA and PAT. In addition, the peak currents of DA and PAT are also significantly enhanced, which are almost three times higher than the same electrode before electropolymerization, demonstrating the improved sensitivity. We also investigated the electrochemical behavior of DA and PAT on pristine MWCNT modified GCE for comparison. It should be pointed out that the peak currents of DA and PAT on MWCNT-BPVCM-*e*/GCE are five times higher than that of pristine MWCNT/GCE (Fig. 3), although similar two corresponding well-defined redox peaks were observed for MWCNT/GCE.

The good electroanalytical response of DA and PAT at the MWCNT-BPVCM-*e*/GCE can be attributed to the following reasons. Firstly, the electropolymerization of carbazole moieties provides a conductive polymeric network on the surface of MWCNT, which enhances the electrical conductivity of MWCNT-BPVCM for more than four times as discussed in the EIS results. As a

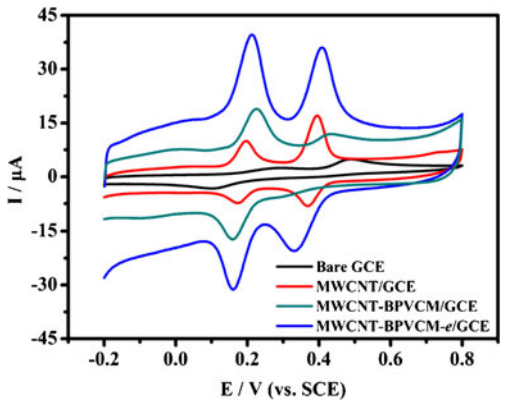

Fig. 3 Cyclic voltammograms (CVs) of 100 μM DA and PAT at a bare GCE, MWCNT/GCE and MWCNT-BPVCM/GCE and MWCNT-BPVCM-*e*/GCE in 0.1 M PBS with scan rate of 100 $mV \cdot s^{-1}$

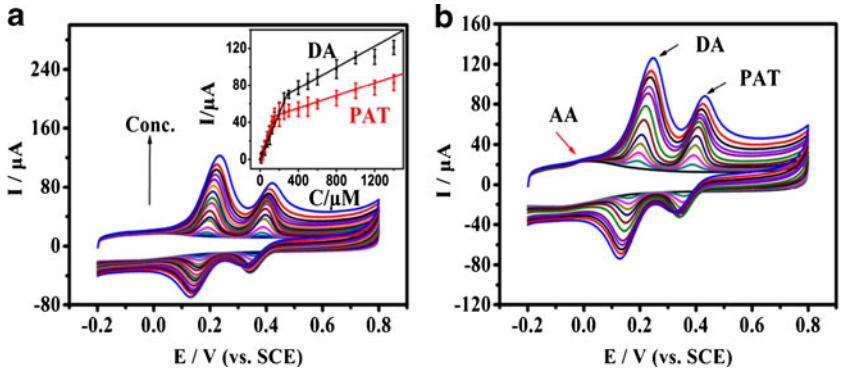

Fig. 4 **a** Simultaneous determination of DA and PAT at the MWCNT-BPVCM-*e*/GCE. Cyclic voltammograms with different concentrations of DA and PAT, the concentrations ranged from 0 to 1000 μM (0, 5, 10, 25, 50, 75, 100, 125, 150, 200, 250, 300, 400, 500, 600, 800, 1000 μM) in 0.1 M PBS. Scan rate: 50 mV · s^{-1}. Inset: plots of the anodic peak current as a function of DA and PAT concentrations. **b** CVs of DA and PAT at the MWCNT-BPVCM-*e*/GCE in the presence of 500 μM AA and 0–1000 μM DA and PAT in 0.1 M PBS. Scan rate: 50 mV · s^{-1}

result, the electron transfer between analytes and electrode was accelerated. Secondly, the carboxyl groups in BPVCM have a strong interact with the amino group of DA and the amide group of PAT, which improve the attraction of DA and PAT toward the electrode and enrich the concentration of the analytes around the electrode (Fig. S5). Thirdly, in contrast to the pristine MWCNT which tend to aggregate into bundles with poor uniformity on the surface of the GCE, the MWCNT-BPVCM composite shows a debundling and well-separated morphology (Fig. S4C and D), providing a big surface area which increases the contact area of the analytes toward the electrode surface.

Effect of scan rate on the electrochemical response of DA and PAT

The effect of scan rate on the anodic peak current (I_{pa}) and the cathodic peak current (I_{pc}) of DA and PAT at the surface of MWCNT-BPVCM-*e*/GCE by CV was studied in 100 μM DA and PAT in pH 7.0 PBS in the range of 25–400 mV · s^{-1} in order to investigate the mechanism of electron transfer and electrode reaction (Fig. S6A). As shown in Fig. S6B and C, I_{pa} and I_{pc} of DA and PAT vary linearly with the scan rate for both analytes, which confirms the adsorption controlled process for electro-oxidation of DA and PAT on the surface of MWCNT-BPVCM-*e*/GCE.

Simultaneous CV determinations of DA and PAT and interference study in the presence of excess AA

The excellent electrocatalytic activity of MWCNT-BPVCM-*e* toward DA and PAT allow us to simultaneously detect DA and PAT by CV. The utilization of the MWCNT-BPVCM-*e*/GCE for the simultaneous determination of DA and PAT was demonstrated by simultaneously changing the concentrations of DA and PAT (Fig. 4a). When the concentrations of both two species increased synchronously, their peak currents increased accordingly. The peak current is linearly related to both DA and PAT concentration over two concentration ranges, DA: 5–300 μM, 300–1000 μM and PAT: 5–150 μM, 150–1000 μM (the inset of Fig. 4a). The detection limit of DA and PAT was estimated to be 2.3 μM and 3.5 μM, respectively. The linear equations were as the follows: DA: (I_{pa} = 0.245 c + 0.847, R^2 = 0.9947, 5–300 μM) and (I_{pa} = 0.055 c + 55.35, R^2 = 0.9903, 300–1000 μM), PAT: (I_{pa} = 0.314 c - 0.736, R^2 = 0.9959, 5–150 μM) and (I_{pa} = 0.031 c + 42.31, R^2 = 0.9904, 150–1000 μM). The slopes of the equations were 0.245 and 0.055 μA · $μM^{-1}$ of DA and 0.314 and 0.031 μA ·

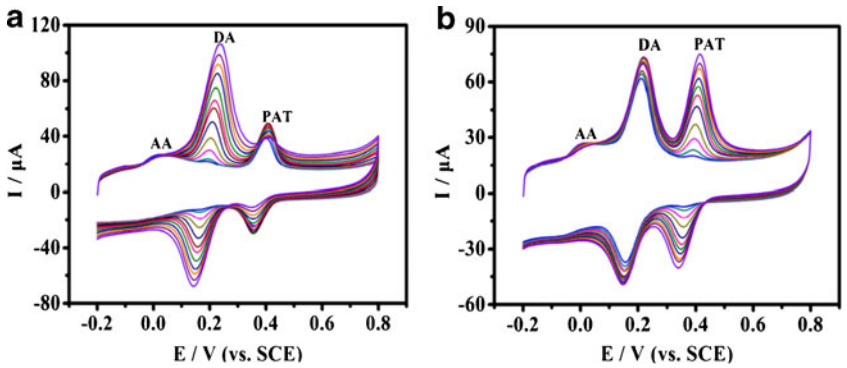

Fig. 5 Cyclic voltammograms of **a** 0–800 μM DA in the presence of 500 μM AA and 100 μM PAT and **b** 0–800 μM PAT in the presence of 500 μM AA and 150 μM DA in 0.1 M PBS at the MWCNT-BPVCM-*e*/GCE. Scan rate: 50 mV · s^{-1}

Table 1 Comparison of previously reported modified electrode with nanocomposite material for the detection limits and linear ranges of DA and PAT

Modified electrode	Detection limit (μmol L^{-1})		Linear range (μmol L^{-1})		Reference
	DA	PAT	DA	PAT	
MWCNT-BPVCM-*e*	2.28	3.48	5–300, 300–1000	5–150, 150–1000	Present work
Pyrolytic carbon	2.3	1.4	18–270	15–225	[10]
ERGO/ZrO_2	NA	NA	9–237	9–231	[9]
graphene	2.64	NA	4–100	NA	[14]
Porous gold nanosheets	0.28	0.23	2–298	3–320	[5]
MWCNT/Q/Nafion	4.72	NA	50–500	NA	[30]

NA not available

μM^{-1} of PAT, respectively. The decreased slopes for both DA and PAT are assumed to be a result of gradual changes in the peak currents of DA and PAT due to the adsorption controlled process transformed to the diffusion controlled process at the electrode surface. Similar phenomenon has been reported by Wang in previous literature [31].

In order to study the effect of interferences, CVs of DA and PAT in the presence of AA were investigated in 0.1 M pH 7.0 PBS. As shown in Fig. 4b, AA shows a very weak peak current at about 0 V on MWCNT-BPVCM-*e*/GCE which is quite separated from the peaks of DA and PAT and thus does not affect the determination of DA and PAT, even the concentration of AA was more than dozen times than that of DA and PAT. The above results showed that the MWCNT-BPVCM-*e*/GCE has a good selectivity for DA and PAT and the presence of AA did not interfere with the detection of DA and PAT. The possible reason of anti-interference of the MWCNT-BPVCM-*e*/GCE toward AA may be that the negatively charged carboxylate group of BPVCM outside the MWCNT repels AA anion and provides a transport channel only for DA and PAT cations, since DA and PAT bear negative charge while AA bears positive charge in 0.1 M pH 7.0 PBS. Some workers have reported that the functionalization of MWCNT with negatively charged polymer improved the anti-interference from AA [32–35]. Fig. S5 shows a scheme of the possible explanation for good anti-interference of MWCNT-BPVCM-*e*/GCE toward AA.

Moreover, in order to further study anti-interferences of the MWCNT-BPVCM-*e*/GCE, we control one variable while keep the other constant. For example, keeping the concentrations of AA and PAT constant, the CVs characterization is performed to investigate the peak current response of DA in the presence of AA and PAT at the MWCNT-BPVCM-*e*/GCE electrode (Fig. 5a). The oxidation peak current density increases with increasing DA concentration, while the responses of AA and PA remain almost unchanged, which demonstrates that AA and PAT have no interfering effect on the detection of DA. And Fig. 5b shows that the presence of AA and DA also has no interfering effect on the detection of PAT. All the results strongly imply that the excellent electrocatalytic activity of MWCNT-BPVCM-*e*/GCE can be used to simultaneous determination of DA and PAT in the interference of AA.

Table 1 shows the electrochemical parameters for determination of DA and PAT compared with the earlier papers. It can be seen that this work presents a wider linear response range and a higher upper detection limit than previously reported nanocomposites modified electrodes for the detection of DA and PAT.

Interference study

The interference of some other substances for detection of DA and PAT is also studied by recording CVs in 0.1 M PBS (pH 7.0) in the presence of 100 μM DA and PAT. In addition to ascorbic acid, other interferents that normally co-exist with DA and PAT in human blood serum or urine have been investigated. A relative error of less than ±5 % is normally regarded as the criterion for interference. The common inorganic ions such as 100-fold Na^+, K^+, Cl^-, CH_3COO^- and CO_3^{2-} have no interference with DA and PAT detection. For organic compounds, 50-fold glucose, lactose, sucrose, urea, and lysine hardly cause interference. However, it should be noted that cysteine and glutathione have a great interference for the detection of DA and PAT. The presence of equal equivalent cysteine and glutathione led to not only great changes in the peak current but also a noticeable shift in the peak potential (Fig. S7). The possible reason is still under investigation.

Real sample analysis

The MWCNT-BPVCM-*e*/GCE was utilized for the simultaneous determination of DA and PAT in pharmaceutical preparations. The DA and PAT concentrations were determined by the calibration method through averaging six repeated measurements at optimum conditions. The analytical results are summarized in Table 2. The good recovery and relative standard deviation (RSD) results of DA in injections and PAT in tablets imply that the modified electrode can be applied to the

Table 2 Determination results of DA and PAT in pharmaceutical preparations

Sample	Added (μM)		Detected (μM)		Recovery (%)		RSD (%)	
	DA	PAT	DA	PAT	DA	PAT	DA	PAT
1	100	100	97.68	93.62	97.68	93.62	3.15	2.23
2	200	200	194.48	189.68	97.24	94.84	2.52	3.85
3	400	400	395.6	379.92	98.90	94.98	2.48	3.23

Average of six determinations at optimum conditions

determination of DA and PAT in the pharmaceutical preparations.

Reproducibility and stability of the MWCNT-BPVCM-e/GCE

The reproducibility of the MWCNT-BPVCM-*e*/GCE was evaluated by CV studies with five independently modified GCE under the same experimental conditions. The result showed an acceptable precision with RSD (relative standard deviation) of 4.13 % and 3.65 % respectively for 100 μM DA and PAT concentration measurements. The repeatability of the electrode was also investigated, where the RSDs were 2.6 % for DA ($n = 5$) and 3.2 % for PAT ($n = 5$) using the same electrode. In order to investigate the long-term stability of the proposed sensor, the MWCNT-BPVCM-*e*/GCE was stored in the air at 25 °C over 2 weeks. The modified GCE retained about 92.6 % of the initial response of DA and PAT, indicating the excellent storage stability of the MWCNT-BPVCM-*e*/GCE.

Conclusions

An electrochemical sensor was successfully applied for the simultaneous determination of DA and PAT using BPVCM functionalized MWCNT. BPVCM is a branched amphiphilic photo-sensitive and electroactive polymer, which can efficiently disperse MWCNT in aqueous solution. The electropolymerization of the carbazole moieties of the BPVCM leads to higher electrocatalytic activity towards the electrooxidation of DA and PAT. DA and PAT can be determined at working potentials of typically 0.21, and 0.39 V (vs. SCE) in the 5 to 1000 μM concentration range with detection limits of 2.3 and 3.5 μM, respectively. In addition, the interference of AA was effectively avoided. The presence of 50-fold glucose, lactose, sucrose, urea, and lysine hardly cause interference. But cysteine and glutathione have a great interference for the detection of DA and PAT. Furthermore, the practicality of the prepared sensor was evaluated by sensing DA and PAT in the pharmaceutical preparations with good recovery results. This analytical range of BPVCM-MWCNTs appears to be wider compared to other materials reported in literatures, which can be considered as promising material for future applications in electrochemical sensing.

Acknowledgments We acknowledge financial support from the National Natural Science Foundation of China (Nos. 51203063 and 21174056), the Fundamental Research Funds for the Central Universities (JUSRP 51305A) and MOE & SAFEA for the 111 Project (B13025).

Compliance with ethical standards The author(s) declare that they have no competing interests.

References

1. Heien M, Khan A, Ariansen J, Cheer J, Phillips P, Wassum K, Wightman M (2005) Real-time measurement of dopamine fluctuations after cocaine in the brain of behaving rats. Proc Natl Acad Sci 102:10023
2. Kachoosangi RT, Wildgoose GG, Compton RG (2008) Sensitive adsorptive stripping voltammetric determination of paracetamol at multiwalled carbon nanotube modified basal plane pyrolytic graphite electrode. Anal Chim Acta 618:54
3. Sanghavi BJ, Wolfbeis OS, Hirsch T, Swami NS (2015) Nanomaterial-based electrochemical sensing of neurological drugs and neurotransmitters. Microchim Acta 182:1
4. Cernata A, Tertişa M, Săndulescua R, Bediouib F, Cristeaf A, Cristea C (2015) Electrochemical sensors based on carbon nanomaterials for acetaminophen detection: a review. Anal Chim Acta 886:16
5. Zhang QL, Feng J, Wang A, Wei J, Lv Z, Feng J (2015) A glassy carbon electrode modified with porous gold nanosheets for simultaneous determination of dopamine and acetaminophen. Microchim Acta 182:589
6. Tsierkezos NG, Ritter U, Thaha YN, Downing C, Szroeder P, Scharff P (2015) Multi-walled carbon nanotubes doped with boron as an electrode material for electrochemical studies on dopamine, uric acid, and ascorbic acid. Microchim Acta. doi:10.1007/s00604-015-1585-6
7. Cheemalapati S, Palanisamy S, Mani V, Chen SM (2013) Simultaneous electrochemical determination of dopamine and paracetamol on multiwalled carbon nanotubes/graphene oxide nanocomposite-modified glassy carbon electrode. Talanta 117:297
8. Kutluay A, Aslanoglu M (2014) An electrochemical sensor prepared by sonochemical one-pot synthesis of multi-walled carbon nanotube-supported cobalt nanoparticles for the simultaneous determination of paracetamol and dopamine. Anal Chim Acta 839:59
9. Vilian AT, Rajkumar M, Chen SM (2014) In situ electrochemical synthesis of highly loaded zirconium nanoparticles decorated reduced graphene oxide for the selective determination of dopamine and paracetamol in presence of ascorbic acid. Colloids Surf B: Biointerfaces 115:295
10. Keeley GP, McEvoy N, Nolan H, Kumar S, Rezvani E, Holzinger M, Cosnier S, Duesberg GS (2012) Simultaneous electrochemical determination of dopamine and paracetamol based on thin pyrolytic carbon films. Anal Methods 4:2048
11. Narayana PV, Reddy TM, Gopal P, Naidu GR (2014) Electrochemical sensing of paracetamol and its simultaneous resolution in the presence of dopamine and folic acid at a multi-walled

carbon nanotubes/poly(glycine) composite modified electrode. Anal Methods 6:9459
12. Liu X, Zhang XY, Wang LL, Wang YY (2014) A sensitive electrochemical sensor for paracetamol based on a glassy carbon electrode modified with multiwalled carbon nanotubes and dopamine nanospheres functionalized with gold nanoparticles. Microchim Acta 181:1439
13. Luo J, Cong J, Fang R, Fei X, Liu X (2014) One-pot synthesis of a graphene oxide coated with an imprinted sol–gel for use in electrochemical sensing of paracetamol. Microchim Acta 181:1257
14. Kim YR, Bong S, Kang YJ, Yang Y, Mahajan RK, Kim JS, Kim H (2010) Electrochemical detection of dopamine in the presence of ascorbic acid using graphene modified electrodes. Biosens Bioelectron 25:2366
15. Li L, Zhou T, Sun G, Li Z, Yang W, Jia J, Yang G (2015) Ultrasensitive electrospun nickel-doped carbon nanofibers electrode for sensing paracetamol and glucose. Electrochim Acta 152:31
16. Luo J, Sun J, Huang J, Liu X (2016) Preparation of water-compatible molecular imprinted conductive polyaniline nanoparticles using polymeric micelle as nanoreactor for enhanced paracetamol detection. Chem Eng J 283:1118
17. Luo J, Fan CH, Wang XH, Liu R, Liu XY (2013) A novel electrochemical sensor for paracetamol based on molecularly imprinted polymeric micelles. Sens Actuators B 909:188
18. De Volder MFL, Tawfick SH, Baughman RH, Hart AJ (2013) Carbon nanotubes: present and future commerical applications. Science 339:535
19. Elouarzaki K, Haddad R, Holzinger M, Giff AL, Thery J, Cosnier S (2014) MWCNT-supported phthalocyanine cobalt as air-breathing cathodic catalyst in glucose/O_2 fuel cells. J Power Sources 255:24
20. Du X, Miao ZY, Zhang D, Fang YX, Ma M, Chen Q (2014) Facile synthesis of β-lactoglobulin-functionalized multi-wall carbon nanotubes and gold nanoparticles on glassy carbon electrode for electrochemical sensing. Biosens Bioelectron 62:73
21. Kang Y, Taton TA (2003) Micelle-encapsulated carbon nanotubes: a route to nanotube composites. J Am Chem Soc 125:5650
22. Datsyuk V, Landois P, Fitremann J, Peigney A, Galibert AM, Soula B, Flahaut E (2009) Double-walled carbon nanotube dispersion via surfactant substitution. J Mater Chem 19:2729
23. Gr schel AH, L bling TI, Petrov PD, Müllner M, Kuttner C, Wieberger F, Müller AH (2013) Janus micelles as effective supracolloidal dispersants for carbon nanotubes. Angew Chem Int Ed 52:3602
24. Haggenmueller R, Rahatekar SS, Fagan JA, Chun J, Becker ML, Naik RR, Krauss T, Carlson L, Kadla JF, Trulove PC, Fox DF, Delong H, Fang Z, Kelley SO, Gilman JW (2008) Comparison of the quality of aqueous dispersions of single wall carbon nanotubes using surfactants and biomolecules. Langmuir 24:5070
25. Prevoteau A, Soulieé-Ziakovic C, Leibler L (2012) Universally dispersible carbon nanotubes. J Am Chem Soc 134:19961
26. Alothman ZA, Bukhari N, Wabaidur SM, Haider S (2010) Simultaneous electrochemical determination of dopamine and acetaminophen using multiwall carbon nanotubes modified glassy carbon electrode. Sens Actuators B 146:314
27. Liu R, Zeng XB, Liu JC, Zheng YY, Luo J, Liu XY (2014) Dispersion of carbon nanotubes in water by self-assembled micelles of branched amphiphilic multifunctional copolymers with photosensitivity and electroactivity. J Mater Chem A 2:14481
28. Ates M, Uludag N (2010) Synthesis and electropolymerization of 9-(4-vinylbenzyl)-9H-carbazole on carbon fiber microelectrode: capacitive behavior of poly (9-(4-vinylbenzyl)-9H-carbazole). Fibers Polym 11:331
29. Gu H, Su XD, Loh KP (2005) Electrochemical impedance sensing of DNA hybridization on conducting polumer film-modified diamond. J Phys Chem B 109:13611
30. Chen PY, Vittal R, Nien PC, Ho KC (2009) Enhancing dopamine detection using a glassy carbon electrode modified with MWCNTs, quercetin, and Nafion. Biosens Bioelectron 24:3504
31. Wang HS, Li TH, Jia WL, Xu HY (2006) Highly selective and sensitive determination of dopamine using a Nafion/carbon nanotubes coated poly (3-methylthiophene) modified electrode. Biosens Bioelectron 22:664
32. Davila MM, Elizalde MP, Mattusch J, Wennrich R (2001) Study of the composite electrodes carbon-polyvinyl chloride and carbon-polyvinyl chloride/Nafion by ex situ and in situ methods. Electrochim Acta 46:3189
33. Zhao H, Zhang YZ, Yuan ZB (2001) Study on the electrochemical behavior of dopamine with poly (sulfosalicylic acid) modified glassy carbon electrode. Anal Chim Acta 441:117
34. Yue Y, Hu GZ, Zheng MB, Guo Y, Gao JM, Shao SJ (2012) A mesoporous carbon nanofiber-modified pyrolytic graphite electrode used for the simultaneous determination of dopamine, uric acid, and ascorbic acid. Carbon 50:107
35. Liu JC, Luo J, Liu R, Jiang JQ, Liu XY (2014) Micelle-encapsulated multi-wall carbon nanotubes with photosensitive copolymer and its application in the detection of dopamine. Colloid Polym Sci 292:153